Preliminary Biomechanical Studies on the Diaphragmatic Function in Control and Patients with Loss of Motor Units

Santos, N. J. G.

November, 2009

Abstract

The main objectives of this thesis are the construction of a three-dimensional (3D) model of the diaphragm and the simulation of the movement of this organ during breathing in normal and pathological cases. The 3D reconstruction of the diaphragm is obtained from segmented images of axial and sagittal views of sectional cuts of a female diaphragm. The finite element analyses of the model are performed during quiet breathing considering three different conditions: a normal diaphragm, a dysfunctional diaphragm caused by amyotrophic lateral sclerosis (ALS) and a diaphragm with a right inactivated hemidiaphragm caused by an unilateral lesion of the phrenic nerve.

Values of the tidal volume and of the maximum axial displacement of the diaphragm are obtained during quiet breathing in all three situations. In the pathological cases these values are significantly smaller than in the normal case, but the volume in the case of ALS patients is larger than in the other pathological case. Thus the impact of the complete right phrenic nerve lesion on the volume is greater than in the ALS case for the same amount of loss of motor units. This suggests that the inspiratory muscles of a patient with such lesion become more activated due to a compensatory response.

Key Words: Diaphragm, 3D Reconstruction, Shell Finite Elements, Hill's Muscle Model, Amyotrophic Lateral Sclerosis, Unilateral Lesion of the Phrenic Nerve.

---

1 Introduction

In the present study normal and pathological functions of the diaphragm are simulated during breathing. The simulation of the movement of the diaphragm is performed using the Finite Element Method (FEM) while the geometrical model of the diaphragm is reconstructed from a cadaver.

In order to obtain a finite element mesh, a geometric model of the diaphragm is needed. This model has to be physiologically accurate and therefore has to be obtained by reconstruction. Models of the diaphragm are widely used in research and the method of reconstruction varies. The existing methods used to reconstruct an object are not very robust because they need various previous assumptions. Almost all of them are user dependent. There are also semi-automatic and automatic techniques but they are very limited. The most used reconstruction technique is semi-automatic. The totally automatic procedure is rarely used because the segmentation of the diaphragm is a very difficult process.

The current reconstruction techniques require medical images of the region of the body where the target organ is, in order to obtain a segmented contour of the organ and to reconstruct the corresponding three-dimensional object. The medical images can be obtained from different sources: (i) x-ray [1], (ii) magnetic resonance [2],[3], (iii) ultrasound [4] and (iv) photography [5],[6]. Each type of image corresponds to different techniques and the procedures to adopt depend on the different human organs and diseases. Radiography, for example, is optimal for bone detection but very poor for soft tissue detection. The most used source images for modelling are magnetic resonance images and photographic images taken from cadavers. Additionally the diaphragm is a very thin structure making its detection in medical images difficult. In the majority of the studies regarding the reconstruction of the diaphragm from medical images, the authors use the contrast between organs, specifically between lungs and abdominal content, to segment the diaphragm. The photographic images consist of cross-sectional photographs of the human body. These images have the advantage of real colour characterization of the body but on the other hand the images have to be taken from cadavers. In corpses the physiology of the body is altered, such as rigidity and absence of tetanic force, and these can change the anatomy of the body.

The diaphragm is a complex three-dimensional organ, both geometrical and mechanically. For this reason, in biomechanical studies, FEM is a good tool for the necessary numerical simulations. Martins *et al* [7][8][9], D'Aulignac *et al* [10] and Pato & Areias [11] used finite element simulations to study the behaviour of skeletal muscles of the human body. In the present work the target of the numerical simulations is the respiration cycle and its consequences in the diaphragm.

The constitutive model adopted in the present study for the diaphragm consists of a modified form of the incompressible transversely isotropic hyperelastic model proposed by Humphrey & Yin [12] for passive cardiac muscles in which the passive and active behaviour of the 1D Hill type model in Pandy *et al* [13] is assigned to the muscle fibres. This new model was proposed and tested by Martins *et al* [9] and improved further by D'Aulignac *et al* [10], Martins *et al* [7][8] and Pato & Areias [11]. The improvements showed to be relevant to model faster contractions, which may occur in intervals of time of the same order of the muscle activation and deactivation times.

The muscle model tries to simulate the behaviour of the skeletal muscles which have a complex mechanical behaviour due essentially to the incompressibility of the tissue and to their single muscle fibre direction. Also activation processes may take place along the muscular fibres due to neural stimulation. The model is a generalization to 3D of the one-dimensional Hill's model. This model is composed of three elements: a (active) contractile element (CE) in series with a (passive) elastic element (SE), both of them in parallel with another (passive) elastic element (PE). The contractile element is the active component of the model, it represents the actin and myosin filaments sliding relative to each other and the active force generated is a result of the number of cross-bridges between the filaments. On the other hand the elastic element SE represents the connective tissue in series with the sarcomeres including the tendon while the PE represents the parallel connective tissue surrounding the contractile element [14].

The diaphragm is modelled as a shell due to its small thickness. The 3D muscle model was therefore simplified to agree with the thin shell theory. In the plane stress case and for a shell without shear deformation $\sigma_{i3} = 0$ ($i = \{1, 2, 3\}$) where the direction 3 of the orthonormal reference frame $(1, 2, 3)$ follows the normal to the middle surface of the shell.

1.1 Diaphragm

The diaphragm is considered the main respiratory muscle responsible for maintaining the correct change in pulmonary volume at the inspiration step of the respiratory cycle because the diaphragm has the highest contribution to the total work performed by all of the inspiratory muscles (about 60 to 80% [15]).

The diaphragm is a musculo-fibrous sheet separating physically and functionally the thorax and the abdomen [16]. It takes the form of the surrounding organs as an elliptical cylindroid capped with a pair of cupolas located on either side of a central plateau. The right cupola is higher than the left one due to the presence of the liver in the right side of the body.

The thoracic and abdominal contents determine the shape of the unstressed dome of the diaphragm creating two separate zones: the diaphragmatic zone, characterized by the two cupolas, and the apposition zone. In the diaphragmatic zone there is a region characterized by a thin, strong aponeurosis of interwoven collagen fibres, called the central tendon or the phrenic centre. This helps the diaphragm to maintain its shape during contraction.

Since the diaphragm acts like a barrier between thorax and abdominal content it is natural to expect some apertures in the muscle for an up to down communication. Aside small gaps there are three main apertures in the diaphragm: (i) the aortic opening, (ii) the oesophageal aperture and (iii) the cava vein aperture.

During quiet breathing the decrease in axial length of the apposed diaphragm (essentially the dome part) is about 1 to 3cm [3],[16], whereas the increase in the sagittal and coronal diameters of the rib cage is only approximately 0.3 to 0.5cm [16], respectively. Therefore the most important change in the diaphragmatic shape during normal quiet breathing occurs when the fibres in the zone of apposition contract and the dome part of the diaphragm descends. This change is responsible for the major part of the variation in volume. Because of this major axial displacement of the domes, the diaphragm is sometimes referred as a piston-like contractile muscle.

The difference in pressure across the diaphragm is known as transdiaphragmatic pressure (Pdi) [17]. It is the total axial force developed by the apposed diaphragmatic fibres divided by their cross-sectional area at the zone of apposition. Each half of the diaphragm is innervated by the right and left phrenic nerves. The phrenic nerve is the only motor supply to the diaphragm and its branches are usually deep within the muscle.

1.2 Pathological Dysfunctions of the Diaphragm

The dysfunctions of the diaphragm addressed in the present study are a consequence of amyotrophic lateral sclerosis (ALS) and of an unilateral complete lesion of the right phrenic nerve. Both these lesions have a similar functional effect on the diaphragm.

ALS causes the degeneration of the upper and lower motor neurons. The neurons cease to send messages to the muscles, causing muscle weakness and atrophy. Although respiratory failure usually occurs as a late event in the course of the disease, this is considered the main cause of death of the patients with ALS. The diaphragm is considered an important determinant of the ALS-related respiratory insufficiency [18]. Studies confirmed that diaphragm weakness in patients with ALS is due to diaphragmatic dysfunction [18].

The ALS symptoms have an insidious onset which originates a long delay from onset to diagnosis. Additionally at the time of diagnosis the respiratory function may already be compromised although pulmonary symptomatology is absent. During disease progression it is essential to evaluate the respiratory

function by conventional tests, nocturnal oxymetry, sleep studies and, sometimes, using neurophysiological techniques [19][20]. Additionally studies showed that the diaphragm dysfunction in ALS is associated with changes in sleep, mainly because the diaphragm is the only inspiratory muscle active during the rapid eye movement (REM) sleep.

The unilateral lesion of the phrenic nerve causes a diaphragm paralysis. Phrenic nerve lesion can be bilateral (a critical condition) or more commonly unilateral, as a result of a thoracic surgical intervention, local compression or inflammatory lesion of the nerve. In an unilateral paralysis of the diaphragm the pulmonary performance is maintained during quite breathing. In fact this phenomenon is corroborated by some studies [21][22][23], although some characteristics and properties of the diaphragm become functionally deteriorated [21][24]. In physical exercise, however, the unilateral paralysis causes a reduction in the performance of the diaphragm [21].

2 Computational Model and Simulation

For the simulation of the movement of the diaphragm during respiration, the first step is the reconstruction of the diaphragm. The diaphragm is a very thin membrane situated at the toraco-abdominal part of the body and its visualization and reconstruction are very difficult to perform. Therefore classical medical images such as MRI, X-ray or ultrasound images are a poor source for the reconstruction. For these reasons real sectional images available and obtained from the Visible Human Project(VHP) [25] were considered.

For the segmentation it was necessary to reformat the axial images of the VHP to sagittal images due to the horizontal shape of some regions of the diaphragm. Therefore these transversal and sagittal sections were necessarily segmented by visual inspection. In each image the contour of the diaphragm was obtained considering the diaphragm as a shell membrane. Several points were identified in the outside line of the diaphragm and splines were generated to create its contour. As a final procedure to generate the model, adjacent spline curves were connected and meshed by interpolation. After the reconstruction an optimization procedure was required to eliminate some artefacts and geometric imperfections detected in the model.

The steps of the segmentation were performed in Rhinoceros™ (generation of splines and interpolation) and Blender (identification of the contours of the diaphragm and optimization). On the other hand Abaqus™ was used to mechanically simulate the respiratory cycle of the different cases under study.

The next step was the definition of the mechanical and physiological aspects of the diaphragm. First the model was divided in three main regions according to their definition on the images of Netter [26]: the central tendon, the muscle and the *inferior tendon*. The *inferior tendon* was defined as the narrow region located along the inferior borders of the diaphragm.

Second, the material properties were assigned to each of the three main regions. The phrenic centre and the *inferior tendon* parts were defined as tendinous tissue. This tendon tissue was considered linearly elastic and isotropic with values for Young's modulus and Poisson's coefficient of 33MPa [5] and 0.33, respectively. The muscle was modelled as in [7][8][11] and its parameters were also taken from [7] and [11], except that a residual activation ($\alpha_{min} = 0.01$) was considered. A constant neural excitation u with a value u_{max} was applied during inspiration. In expiration the value of u was set to zero. The diaphragm was considered as an homogeneous shell object with a thickness of 3mm for the tendon and 5mm for the muscle [5].

The boundary conditions were imposed mainly in the borders of the model. On the boundaries of the

inferior tendon the diaphragm was constrained along the three spatial directions, although there is a relative movement of the diaphragm during breathing. The fixation of the borders is a simplification due to the relative complexity of the movement. The apertures and openings of the diaphragm were constrained along the sagittal and the coronal axis while the axial displacement was kept free. The rotational movement was also kept free in the previous boundaries, except for the lateral and anterior zones which can not rotate about the sagittal and the coronal axes, respectively. Finally the pillars of the diaphragm were totally constrained along the six spatial and rotational degrees of freedom.

The load type considered in the simulations was the pressure. The value of the pressure between the inside and the outside (Pdi) considered in this study, for a normal and quiet breathing, was $5cmH_2O$ [27]. This value was assigned to the two previously separated regions of the diaphragm: the apposition and the diaphragmatic zones. In the inspiration (expiration) the pressure in the apposition zone points to the outside (inside) and in the diaphragmatic zone points downwards (upwards).

The solid object was meshed in Abaqus™, with S3 triangular shell finite elements with only one integration point.

2.1 Determination of the Direction of the Fibres

The initial direction of the fibres is an input for the muscle model considered in this study. The vector which describes the direction of the fibres has to be normalized and to be located in the plane of each triangular element.

The initial direction of the fibres has a radial pattern, starting in the tendon of the phrenic centre and ending at the inferior borders of the diaphragm. The directions were determined in a routine implemented in Fortran. In each element a vector was obtained. This vector is the projection of the fibre direction on the plane of the element. Each fibre direction is defined by a vector containing the integration point of each element and a fixed point located sufficiently above and on a vertical axis passing by the centre of the central tendon.

2.2 Breathing Tests

The simulation of the behaviour of the diaphragm in the respiratory cycle was performed under a normal tidal breathing. The inspiration lasts 2 seconds while the expiration lasts 3 seconds [6]. Three main analyses were performed: (i) a tidal breathing; (ii) a breathing simulating a respiratory cycle in a patient with ALS with 50% loss of randomly distributed motor units of the diaphragm; and finally (iii) a breathing with right inactivated muscle fibres that simulate the respiration of a patient with a complete lesion of the right phrenic nerve. Also several simulations were performed during normal inspiration to study the behaviour of the diaphragm for different values of u_{max}.

The results obtained from the analyses provided relevant information for later interpretation and possible comparisons. Qualitatively, the behaviour of the diaphragm in the simulations was described. Quantitatively, the absolute value of the maximum axial displacement (MAD) of the diaphragm and the variation of the volume were also obtained.

The volume variation was calculated as the difference between two fictitious volumes: one obtained from the initial shape of the diaphragm and the other from its deformed configuration in a later phase of the

respiration. At each instant of the analysis the volume of the diaphragm was evaluated as the sum of all the volumes under each element of the model relatively to a fixed horizontal plane.

3 Results

The reconstructed geometrical model of the diaphragm and the corresponding finite element mesh are presented in Figure 1.

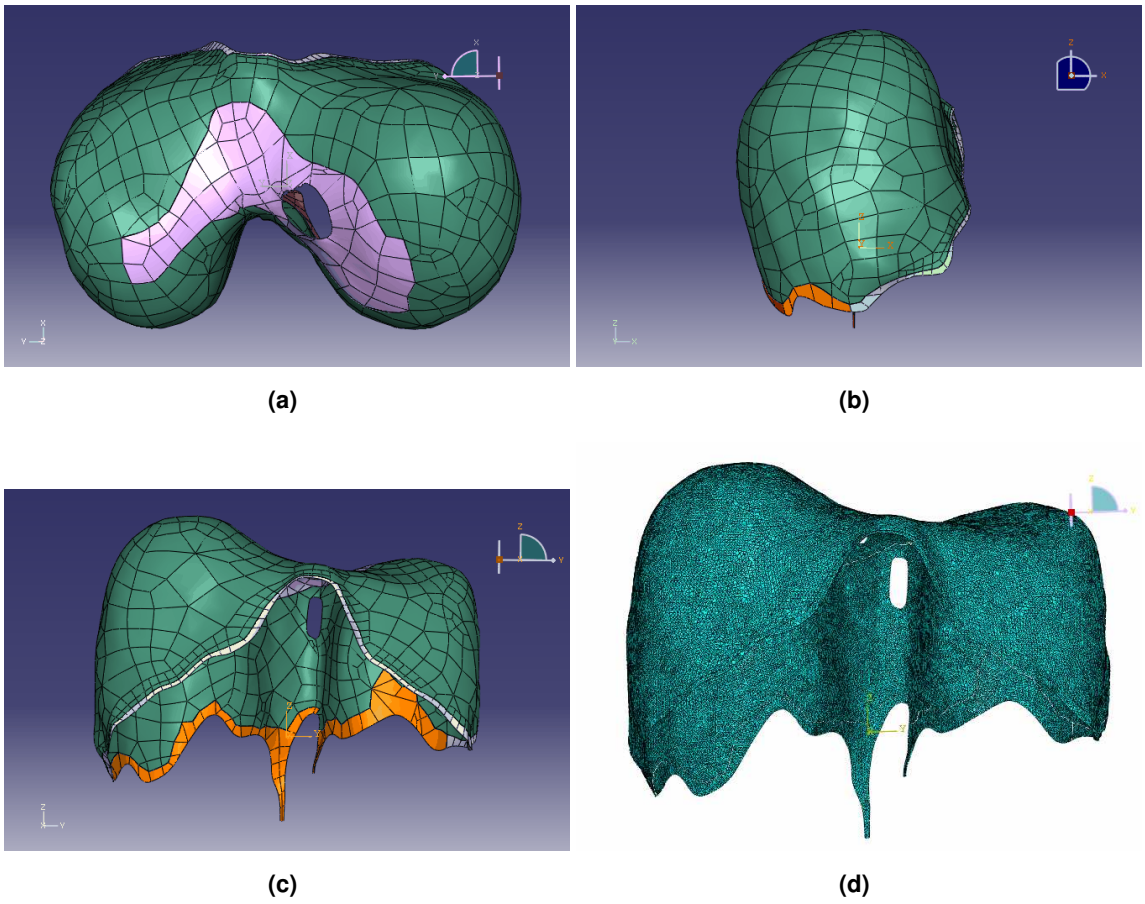

Figure 1: Geometric model of the diaphragm: axial (a), sagittal (b) and coronal (c) views, and the finite element mesh (d).

3.1 Variation of the neural excitation

In the present study FEM analyses of the of the diaphragm during inspiration were performed considering different values of u_{max} in the excitation function $u(t)$. The main objective of these analyses was to characterize and to determine the influence of the value of u_{max} in the respiration. Indeed in a quiet normal breathing the level of excitation of the diaphragm by the phrenic nerve is still unknown. In Table 1 the results obtained from the analyses performed with different values of u_{max} varying between 0% and 100%

are presented. For each u_{max} the tidal volume (TV) and the MAD of the top part of the diaphragm were calculated.

u_{max} (%)	TV (cm^3)	MAD (mm)
0	7.529	0.15
10	390.516	6.95
20	519.721	9.37
30	564.182	10.55
40	619.428	11.37
50	644.177	11.88
60	661.823	12.24
70	675.497	12.51
80	685.449	12.73
90	693.239	12.90
100	703.000	13.04

Table 1: Tidal volume (TV) and absolute value of the maximum axial displacement (MAD) at the top of the diaphragm for different values of u_{max}.

The values of the TV evolve approximately between 390cm^3 and 700cm^3 when u_{max} is increased. The evolution of the TV is not linear: for small u_{max} the volume is smaller but increases rapidly, and for larger values of u_{max} the TV is also large but the values seem to stabilize. The evolution of the value of MAD is similar. Its values vary approximately between 7mm and 13mm. When the excitation u is zero the muscle fibres are not activated. Considering the small values of the volume and of the displacement at a zero excitation it is possible to conclude that the activation term in the constitutive equation is responsible for the majority of the deformation of the diaphragm.

The values given in the literature [6] and the results obtained for TV and MAD suggest that the best interval of u_{max} to characterize the excitation in a normal quiet breathing is between 20 and 30%. It is important to stress that when the contraction of the muscle of the diaphragm increases, the Pdi also increases, but this variation in Pdi was not considered.

3.2 Normal and Pathological Breathing

The normal and pathological quiet breathing were simulated performing FEM analyses with a value of u_{max} equal to 30%. In the inspiration the muscle of the diaphragm contracts, the domes of the diaphragm descend and its apposition and its anterior and posterior zones shrink. The horizontal displacements of the diaphragm, as a consequence of the contraction of the muscle, are smaller in comparison with the axial displacement of the domes. The posterior zone of the diaphragm has a smaller contraction in comparison with the displacement of the apposition and anterior parts of the diaphragm. The differences between the three cases are mainly related to the tidal volume, the descent of the domes and the values of the displacements as a consequence of the contraction. On the normal and ALS cases the decrease in height of the domes is larger in the right dome. On the right inactivated hemidiaphragm case the left side of the diaphragm suffers larger displacements comparatively to the right side and consequently the decrease in height of the domes

is larger in the left dome. On the pathological cases the displacements due to the contraction of the fibres are small in the regions where the fibres are inactivated.

In the expiration the diaphragm has a quasi-symmetric behaviour relatively to the inspiration. Generally the domes ascend and the lateral sides of the diaphragm move to the outside. These movements characterize the relaxation of the diaphragmatic muscle.

The evolution in time of the volume under the diaphragm and of the MAD is identical in the three simulated cases (see Figure 2). The main difference in the volume and displacement profiles between the normal and the pathological cases is their values. The TV is approximately 564cm^3, 306cm^3 and 196cm^3 and the MAD at the end of inspiration is about 10.6mm, 5.55mm and 5.74mm, in the normal, ALS and right inactivation of the hemidiaphragm cases, respectively.

In all cases, both variations have four zones during breathing. In the inspiration, all the variation in volume and displacement takes place approximately at the first second of the analysis. Similarly in the expiration, all the variation occurs approximately during the first one and a half seconds. During these periods the evolution has a quasi-exponential behaviour. At the remaining period of time the variation is inexistent. This suggests that the time duration is probably smaller because the diaphragmatic muscle, in inspiration, and the expiratory muscles, in expiration, require a shorter period of time to contract. On the other hand the periods of time during inspiration and expiration where there is no variation may represent the periods of gas exchange in the lungs and of muscle relaxation.

The tidal volume in the pathological cases is lower than in the normal breathing as expected. Nevertheless the volume of the ALS case is approximately 110cm^3 larger than in the case of a right inactivated hemidiaphragm. It is known that the effect of the inactivation of the fibres in one of the hemidiaphragms is not significant in the performance of the quiet breathing. However the small amount of volume exchanged during breathing indicates that the lungs are not being well ventilated. This suggests that, in the case of an inactivated hemidiaphragm and in view of medical knowledge retrieved from clinical cases, there is an active compensation from the other inspiratory muscles or even from a reinforcement of the healthy fibres of the diaphragm. This phenomenon, however, does not occur in a ALS patient because the disease usually affects the other respiratory muscles preventing a possible compensation. The value of the MAD of the diaphragm is similar in both pathological cases and smaller than in the healthy case, although in the right inactivated diaphragm case it is located in the left dome.

The maximum-in-plane stress values vary along the surface of the diaphragm in the three cases. The values of this stress in the muscle and in the tendon are different: the stress is greater in the tendinous regions. The values of this stress in the muscle are approximately two times smaller than in some regions of the phrenic centre and of the inferior tendon. In the three cases the values of the maximum-in-plane stress in the activated fibres of the muscle are approximately constant at each instant of time. At the end of inspiration the value of the maximum-in-plane stress in the activated fibres is 0.5309MPa while in the pathological cases the inactivated fibres become stress free as expected. In the muscle the direction of the maximum-in-plane stress is approximately the same as the direction of the muscle fibres.

In the tendon the maximum-in-plane stress ranges approximately between $-0.2MPa$ and $2MPa$ in normal breathing and between $-0.1MPa$ and $1MPa$ in both pathological cases, at the end of inspiration. The orientation of the maximum-in-plane stress in the tendon is less organized comparatively to the muscle but in the regions where the tendon contacts the muscle, the orientation of this stress is approximately the same as in the muscle. Additionally in both pathological cases the orientation is generally more chaotic in

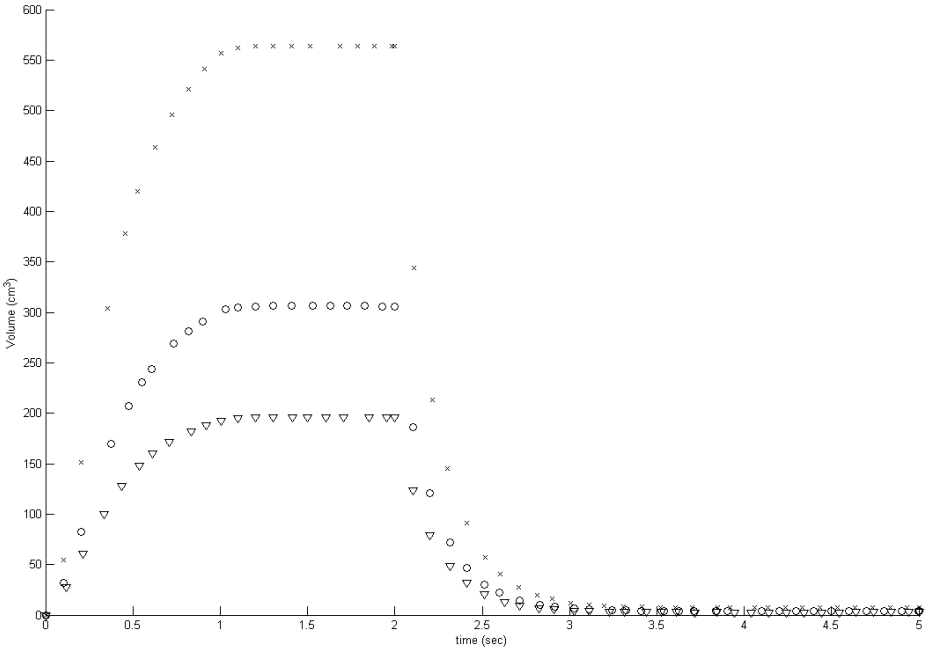

(a)

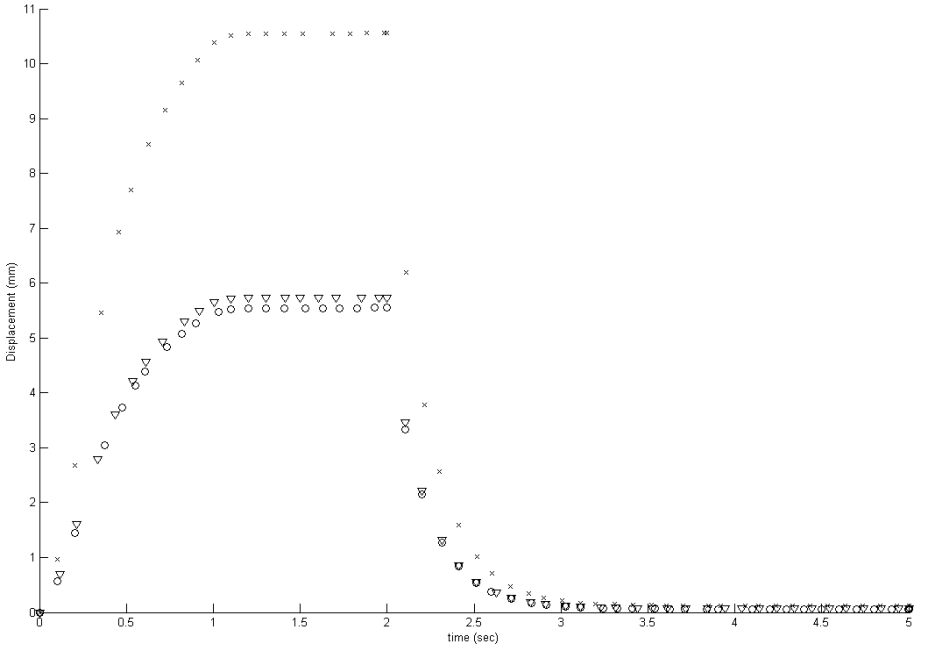

(b)

Figure 2: Variation of the volume (a) and of the absolute value of the maximum axial displacement (b) with time, in the normal breathing ($\circ$), in ALS ($\times$) and right inactivation of the hemidiaphragm (∇).

comparison with the normal case.

4 Conclusion and Future Developments

In this work, computational simulations of the mechanical behaviour of the diaphragm in healthy and pathological conditions were performed. A three-dimensional geometric model of the diaphragm obtained from medical images taken from a female cadaver (VHP) was constructed. A constitutive model for 3D skeletal muscles that incorporates both passive and active behaviours was adopted to characterize the diaphragm. The tendon was assumed to be linear elastic and isotropic.

A finite element mesh with triangular shell elements was generated and the muscle behaviour was incorporated in Abaqus™ package by implementing a UMAT subroutine. After providing the data relative to the material properties of the tissues involved, imposing boundary and initial conditions and applying a pressure in the outer surface of the diaphragm, several numerical simulations were performed.

A parametric study of the constant value of the neural excitation (u_{max}) to be applied during inspiration was carried out. Results for the variation of the volume between the current and the initial configurations, for the MAD of the diaphragm and for the stresses were obtained in healthy and pathological conditions during a 5 seconds long quiet breathing. The pathological conditions considered correspond to patients with a diaphragmatic dysfunction due to ALS and with a right inactivated hemidiaphragm caused by a complete lesion of the right phrenic nerve.

As future developments, it is proposed that the reconstruction of the diaphragm of the male cadaver should also be performed. In the VHP the male specimen is significantly younger than the female donor considered in this work. Additionally, the diaphragm can present significant anatomical differences in view of the gender.

The diaphragm has a movement relative to the body as a consequence of the movement of the other inspiratory muscles and ribs. A more accurate analysis should be considered by allowing the borders of the diaphragm during respiration to displace. The values of the displacement of the inferior borders of the diaphragm should be experimentally determined from medical imaging of a quiet breathing or from the literature. It is important to refer that in this case the volume has to be differently determined. Indeed the procedure used in this work to calculate the volume is based on the fact that the diaphragm is fixed in a closed curve at all times.

It would also be important to consider different and eventually more regions to apply the pressure. This requires a more detailed description of the Pdi on the surface of the diaphragm.

References

[1] A. Condurache, T. Aach, K. Eck, J. Bredno, and T. Stehle, “Fast and robust diaphragm detection and tracking in cardiac x-ray projection images,” *Proceedings of the SPIE*, vol. 5747, pp. 1766–75, 2005.

[2] L. Hoyte, L. Schierlitz, K. Zou, G. Flesh, and J. R. Fielding, “Two- and 3-dimensional mri comparison of levator ani structure, volume, and integrity in women with stress incontinence and prolapse,” *American Journal of Obstetrics and Gynecology*, vol. 185, no. 1, pp. 11–9, July 2001.

[3] E. Promayon and L. Gaillard, “Modèle fonctionnel du diaphragme pour l’acquisition et le diagnostic en imagerie médicale,” Tech. Rep., 2002/2003.

[4] M. Quaranta, C. Salito, E. Magalotti, P. Monaco, C. Forlani, A. Pedotti, and A. Aliverti, “Non-invasive three-dimensional imaging of human diaphragm in-vivo,” *Engennering in Medicine and Biology Society*, pp. 5278–81, August 2008.

[5] M. Behr, L. Thollon, P.-J. Arnoux, T. Serre, S. V. Berdah, P. Baque, and C. Brunet, “3d reconstruction of the diaphragm for virtual traumatology,” *Surg Radiol Anat*, no. 28, pp. 235–40, February 2006.

[6] W. P. Segars, D. S. Lalush, and B. M. Tsui, “Modeling respiratory mechanics in the mcat and spline-based mcat phantoms,” *IEEE Transactions on Nuclear Science*, vol. 48, no. 1, pp. 89–97, February 2001.

[7] J. A. C. Martins, M. P. M. Pato, and E. B. Pires, “A finite element model of skeletal muscles,” *Virtual and Physical Prototyping*, vol. 1, no. 3, pp. 159–70, September 2006.

[8] J. A. C. Martins, M. P. M. Pato, E. B. Pires, R. M. N. Jorge, M. Parente, and T. Mascarenhas, “Finite element studies of the deformation of the pelvic floor,” *Annals of the New York Academy of Sciences*, vol. 1101, pp. 316–34, 2007.

[9] J. A. C. Martins, E. B. Pires, R. Salvado, and P. B. Dinis, “A numerical model of passive and active behaviour of skeletal muscles,” *Computer Methods in Applied Mechanics and Engineering*, no. 151, pp. 419–33, 1998.

[10] D. D’Aulignac, J. A. C. Martins, E. B. Pires, T. Mascarenhas, and R. M. N. Jorge, “A shell finite element model of the pelvic floor muscles,” *Computer Methods in Biomechanics and Biomedical Engineering*, vol. 8, no. 5, pp. 339–47, October 2005.

[11] M. P. M. Pato and P. M. A. Areias, “Active and passive behavior of soft tissues: pelvic floor muscles,” *Communications in Numerical Methods in Engineering*, 2009, (Accepted).

[12] J. D. Humphrey and F. C. P. Yin, “On constitutive relations and finite deformations of passive cardiac tissue: I. a pseudostrain-energy function,” *ASME Journal of Biomechanical Engineering*, no. 109, pp. 298–304, 1987.

[13] M. G. Pandy, F. E. Zajac, E. Sim, and W. S. Levine, “An optimal control model for maximum-height human jumping,” *Journal of Biomechanics*, vol. 12, no. 23, pp. 1185–98, 1990.

[14] A. Ratnovsky, U. Zaretsky, R. J. Shiner, and D. Elad, “Integrated approach for in vivo evaluation of repiratory muscles mechanics,” *Journal of Biomechanics*, no. 36, pp. 1771–84, May 2003.

[15] A. Ratnovsky and D. Elad, “Anatomical model of the human trunk for analysis of respiratory muscles mechanics,” *Respiratory Physiology & Neurobiology*, no. 148, pp. 245–62, 2005.

[16] G. R. Harrison. Springer London, 2005, ch. The Anatomy and Physiology of the Diaphragm, pp. 45–58.

[17] A. M. Boriek, N. G. Kelly, J. R. Rodarte, and T. A. Wilson, "Biaxial constitutive relations for the passive canine diaphragm," *J Appl Physiol*, no. 89, pp. 2187–90, July 2000.

[18] T. Similowski, V. Attali, G. Bensimon, F. Salachas, S. Mehiri, I. Arnulf, L. Lacomblez, M. Zelter, V. Meininger, and J.-P. Derenne, "Diaphragmatic dysfunction and dyspnoea in amyotrophic lateral sclerosis," *Eur Respir Journal*, no. 15, pp. 332–7, 2000.

[19] P. L. Schiffman and J. M. Belsh, "Pulmonary function at diagnosis of amyotrophic lateral sclerosis. rate of deterioration." *CHEST*, vol. 166, no. 103, pp. 508–13, 1993.

[20] H. Stewart, A. Eisen, J. Road, M. Mezei, and M. Weber, "Electromyography of respiratory muscles in amyotrophic lateral sclerosis," *Journal of the Neurological Sciences*, vol. 191, pp. 67–73, 2001.

[21] C. M. Laroche, A. K. Mier, J. Moxham, and M. Green, "Diaphragm strength in patients with recent hemidiaphragm paralysis," *Thorax*, vol. 43, pp. 170–4, 1988.

[22] J.-P. Marie, C. Tardif, Y. Lerosey, J. Gibon, M. Hellot, M. Tadié, J. Andrieu-Guitrancourt, D. Dehesdin, and P. Pasquis, "Selective resection of the phrenic nerve roots in rabbits. part ii: Respiratory effects," *Respiration Physiology*, vol. 109, pp. 139–48, 1997.

[23] J.-P. Marie, Y. Lacoume, A. Laquerrière, C. Tardif, J. Fallu, G. Bonmarchand, and E. Verin, "Diaphragmatic effects of selective resection of the upper phrenic nerve root in dogs," *Respiratory Physiology & Neurobiology*, vol. 154, pp. 419–30, 2006.

[24] C. Shindoh, W. Hida, H. Kurosawa, S. Ebihara, Y. Kikuchi, T. Takishima, and K. Shirato, "Effects of unilateral phrenic nerve denervation on diaphragm contractility in rat," *Tohoku J. Exp. Med.*, vol. 173, pp. 291–302, 1994.

[25] M. J. Ackerman, "The visible human project," *Proceedings of the IEEE*, vol. 86, no. 3, pp. 504–11, March 1998.

[26] F. H. Netter, "Atlas interativo de anatomia humana," Software, Novartis Medical Education, 1999.

[27] M. J. Tobin, L. Brochard, and A. Rossi, "Assessment of respiratory muscle function in the intensive care unit," *Am J Respir Crit Care Med*, vol. 166, no. 10, pp. 610–23, 2002.